

Recirculation of Inhaled Xenon Does Not Alter Lung CT Density¹

Jeffrey B. Hoag, Matthew Fuld, Robert H. Brown, Brett A. Simon

Rationale and Objectives. Xenon-enhanced computed tomography (Xe-CT) measures regional ventilation from changes in lung parenchymal CT density during the multibreath washin/washout of inhaled Xe gas. Because Xe is moderately soluble, vascular uptake and redistribution has been proposed as a confounding phenomenon. We propose that the redistribution of Xe via the circulation is negligible, and correction is unwarranted.

Materials and Methods. Unilateral ventilation with 60% Xe was performed in intubated canines. Whole-lung CT images were obtained at baseline and after 1 and 5 minutes of unilateral Xe ventilation. Comparisons between blocked (B) and Xe ventilated (V) whole lung densities were made. Density of paraspinous muscle and blood (aorta, inferior vena cava) were also compared.

Results. The density of lung tissue in the V lungs increased significantly compared to B lungs after 1 minute (B -688.5 ± 54.3 Hounsfield units [HU] vs. V -535.4 ± 55.6 HU, $P < .05$) and 5 minutes (B -689.1 ± 52.2 HU vs. V -492.9 ± 89.1 HU, $P < .05$) of Xe ventilation. The density in the blocked lungs did not significantly change after either 1 or 5 minutes of ventilation with Xe. Although density tended to increase with time in the blood and muscle, the change only reached significance in muscle at 5 minutes.

Conclusions. Five minutes of ventilation with a high concentration of Xe does not cause measurable density changes in the contralateral, unventilated lung. Xe accumulation in muscle tissue limits redistribution. Correction of Xe-CT time-series density data may be unnecessary.

Key Words. Xenon-enhanced computed tomography; regional lung ventilation; xenon redistribution.

© AUR, 2007

Xenon-enhanced computed tomography (Xe-CT) has been used to measure regional pulmonary ventilation by determining the washin and washout rates of stable xenon gas. Early models of Xe-CT made the assumption that Xe was insoluble in blood and tissue, giving rise to mono-exponential washin or washout curves (1,2). Although Xe gas

is inert, it is moderately soluble in the blood (solubility coefficient = 0.115) (3). The anesthetic properties and the utility of Xe for CT-based cerebral perfusion measurements depend on this solubility of Xe gas in the blood, therefore leading to the suggestion that these early models were oversimplifications.

Because of this measurable gas uptake, it has been proposed (4,5) that Xe uptake in the lungs, storage of dissolved Xe in the blood and peripheral tissues, and subsequent recirculation back to the lung may affect both background levels or alveolar accumulation rates. These models propose that the levels of Xe gas in the lung, which ultimately determine the CT-density signal, are composed of essentially four compartments. The first and second arise from the air component, made up of the inspired concentration of Xe and the concentration of Xe

Acad Radiol 2007; 14:81-84

¹ From the Division of Pulmonary and Critical Care Medicine, Department of Medicine (J.F.B., B.A.S.) and Department of Anesthesiology and Critical Care Medicine (M.F., R.H.B., B.A.S.), Tower 711, The Johns Hopkins University, 600 N. Wolfe Street, Baltimore, MD 21287-8711. Received September 29, 2006; accepted October 20, 2006. These experiments were supported by grants from The National Institutes of Health (NIH HL64368, HL073994) and The Department of Defense (DAMD17-02-1-0732). **Address correspondence to:** J.B.H. e-mail: bsimon@jhmi.edu

© AUR, 2007

doi:10.1016/j.acra.2006.10.012

already in place in the alveoli. The third and fourth are vascular contributions, including blood uptake from of Xe into the pulmonary venous blood and the pulmonary arterial delivery of recirculated Xe in returning blood flow. Kreck et al (5) proposed this four-compartment model, making complex mathematical corrections to account for the influences of each on the lung CT density measured during Xe washin and washout.

We hypothesize that redistribution of Xenon via the circulation back to other regions of the lung is negligible, and mathematical modeling of Xe recirculation in Xe-CT imaging is unwarranted. Using a canine model of single-lung ventilation with a high concentration of Xe gas, we assessed the degree of vascular redistribution of inhaled Xe to the nonventilated lung.

MATERIALS AND METHODS

This protocol was approved by the Johns Hopkins University Animal Care and Use Committee. All animal studies were performed within the guidelines for care defined by the American Physiological Society and the National Institutes of Health.

Animal Preparation

Male mongrel canines (20–25 kg, $n = 3$) were anesthetized with pentobarbital and relaxed with pancuronium. Endotracheal intubation (9.0 mm i.d.) was performed and an Arndt bronchial blocker (Cook Critical Care, Bloomington, IN) was placed in the left or right mainstem bronchus (randomized) under bronchoscopic guidance. Eucapnic ventilation was maintained with a Harvard piston pump respirator. Xenon gas was delivered via a specialized mixing device (Enhancer 3000, Diversified Diagnostic Products, Houston, TX) that maintained constant Xe concentration (60% Xe, 35% O₂) while recycling exhaled Xe gas in closed circuit. At the conclusion of each study, the animals were awakened from anesthesia, extubated, and all recovered uneventfully.

Image Acquisition

All scans were performed on a Siemens Somatom IV scanner during a functional residual capacity breath-hold. Scanner settings were 80 kV, 255 mA, 512 × 512, helical scan reconstructed in 3-mm slice thickness. Before the start of the protocol, the lungs were inflated to total lung capacity (30 cmH₂O airway pressure) for 30 seconds to minimize atelectasis. CT images were obtained at four

time points: 1) baseline with balloon down, 2) baseline with balloon up, 3) 1 minute after ventilation with 60% Xe to the nonblocked lung, and 4) 5 minutes ventilation with 60% Xe to the nonblocked lung.

Image Analysis

The images were transferred to PC workstations and analyzed using customized software (PASS) from the University of Iowa, Division of Physiologic Imaging (6). Each slice was semiautomatically segmented to separate lung tissue from chest wall and mediastinum. Left and right lungs were analyzed separately to determine total lung volume and mean lung density at each time point. In addition, inferior vena cava (IVC) and paraspinal muscles were obtained from randomly selected regions in 10 slices through the chest.

Statistical Analysis

Data from each time point were compared using a one-way analysis of variance within each group. Data from groups were compared using Student's *t*-test at each time point. Values are expressed in Hounsfield units (HU) as means ± standard deviation. Significance was determined from $P < 0.05$.

RESULTS

There was good lung separation with the bronchial blocker as evidenced by auscultation, maintenance of lung volume by CT, and confirmed by no immediate entry of Xe into the blocked lung by CT. Over the course of each experiment, there was an increase in density of the Xe-ventilated lung, whereas the density of the blocked lung was unchanged. Representative images obtained from a single animal during the control period with the balloon up, and at 1 and 5 minutes after unilateral ventilation with 60% Xe (Fig 1) show a progressive increase in density in the Xe-ventilated lung with no appreciable change in the blocked, non-ventilated lung.

Figure 2 displays no change in density data from the ventilated versus the blocked lung. In the blocked lung, there is no change density over the 5 minutes of Xe ventilation and no change from baseline (baseline: -680.6 ± 65.6 HU, 1 minute Xe: -688.5 ± 54.3 HU, 5 minute Xe: -689.1 ± 52.1 , $P = .93$). At 1 and 5 minutes, there is a significant increase in lung density in the ventilated lung compared with baseline (baseline: -662.3 ± 28.8 HU, 1 minute Xe: -535.4 ± 55.6 HU, 5 minute Xe: $-492.9 \pm$

CT Imaging after Xe Ventilation:

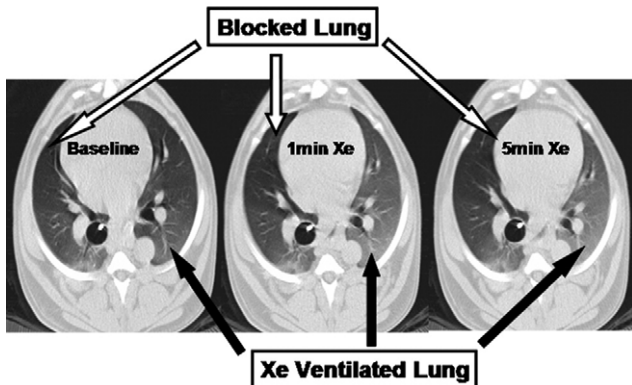


Figure 1. Representative computed tomography images from one canine: the Arndt bronchial blocker catheter is visible in the right mainstem bronchus. Note the increased density (lighter gray) in the left (ventilated) lung at 1 and 5 minutes after xenon ventilation, with no appreciable change in the blocked lung.

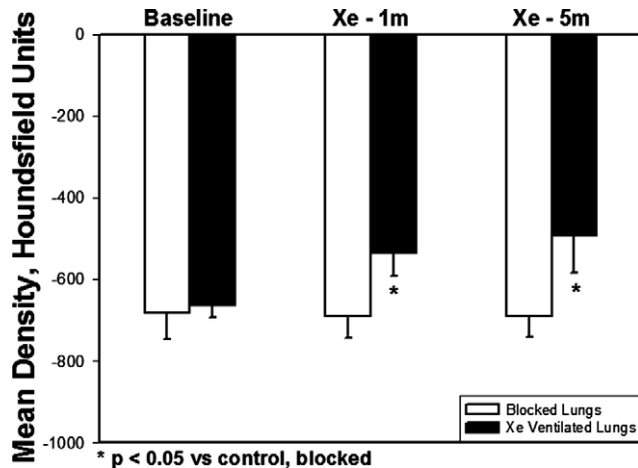


Figure 2. Mean density (Hounsfield unit) of lung tissue in ventilated and blocked lungs at baseline and 1 and 5 minutes of unilateral xenon ventilation.

89.1, $P = .039$) and when compared with the blocked lung at the same time (baseline: -680.6 ± 65.6 HU vs. -662.3 ± 28.8 HU, $P = .68$; 1 minute Xe: -688.5 ± 54.3 HU vs. -535.4 ± 55.6 HU, $P = .03$; 5 minute Xe: -689.1 ± 52.1 vs. -492.9 ± 89.1 , $P = .03$).

Figure 3 shows the density of paraspinal muscles, aorta, and inferior vena cava at baseline and after 1 and 5 minutes of Xe ventilation. With increased duration of ventilation with Xe, the density of the blood and muscle increased modestly, reaching statistical significance only in the muscle compartment after 5 minutes (baseline 58.7 ± 6.0 vs. 5 minutes 67.8 ± 6.7 HU).

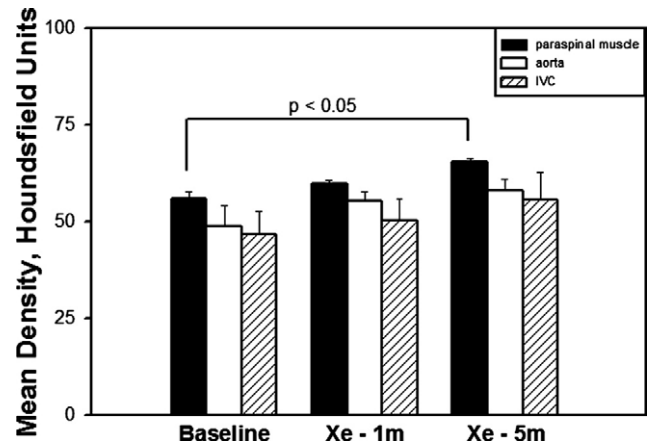


Figure 3. Mean computed tomography tissue density (Hounsfield unit) in paraspinal muscle, aorta, and inferior vena cava at baseline and 1 and 5 minutes of unilateral xenon ventilation.

DISCUSSION

The calculation of regional ventilation from the washin or washout of the radiodense tracer gas Xe requires the construction of a model of the process with requisite assumptions. Although Xe has a modest solubility in blood (3), its uptake does have physiologic significance, as evidenced by its use to measure cerebral blood flow (7,8) and its anesthetic effects (9). Early models ignored this solubility and some also assumed the washin and washout processes were identical, taking advantage of the additional information available in the steep portion of the curves to improve signal-to-noise ratio (1–2, 10–11). Subsequent studies have identified differences in the washin and washout time constants that may be related to gas density and airway branching structures (4) and used the uptake of Xe by the pulmonary blood flow to estimate regional ventilation/perfusion relationships (5). Both of these studies also identified recirculation of Xe as a possible confounder and either adjusted their imaging protocol (4) or model (5) to account for it.

We examined changes in CT lung density during unilateral ventilation with a high concentration of inspired Xe to assess the potential for Xe recirculation via the blood to the contralateral lung. Typical length of Xe inhalation in an animal Xe-CT study is 30–50 breaths (2–3 minutes); therefore, we followed the density changes over a 5-minute period of a high concentration of inspired Xe to ensure adequate time for recirculation of Xe if it were to occur. In this model, designed to maximize conditions for Xe recirculation, prolonged one-lung ventilation with Xe did not lead to a measurable increase in contralateral

lung density. There was, over time, an increase in the density of the paraspinal muscles after ventilation with Xe. Likely, skeletal muscle and fat serve as a large sink or reservoir for absorbed Xe such that return of Xe to the lung during the washout phase is not detectable.

A second potential impact of Xe uptake is the change in density of the blood and/or lung tissue due to Xe absorption. If one liberally considers that blood density increases as much as 10 HU during prolonged Xe inhalation and that normal lung is 20%–40% tissue (–800 to –600 HU), then even if the tissue were all blood the density of the parenchyma would increase at most 2 to 4 HU, less than the typical noise seen in the Xe-CT signal.

It is important to continually refine our physiologic models and examine the validity of their explicit and implicit assumptions. However, for the case of Xe uptake and recirculation in Xe-CT ventilation measurements, our data suggest that there is no significant impact on the measured lung time-density curves. Because of this, we believe that incorporation of Xe recirculation in mathematical models of Xe washin/washout is unnecessary.

ACKNOWLEDGMENTS

The authors thank Ms. Bea Mudge for expert CT scanning and Drs. Eric Hoffman and Junfeng Guo of the Univer-

sity of Iowa, Division of Physiologic Imaging, for the use of PASS (Pulmonary Analysis Software Suite) software.

REFERENCES

1. Simon BA, Marcucci C, Fung M, et al. Parameter estimation and confidence intervals for Xenon-CT ventilation studies: a Monte Carlo approach. *J Appl Physiol* 1998; 84:709–716.
2. Marcucci C, Nyhan D, Simon BA. Distribution of regional pulmonary ventilation in prone and supine dogs using xenon enhanced CT. *J Appl Physiol* 2001; 90:421–430.
3. Goto T, Suwa K, Uezono S, et al. The blood-gas partition coefficient of xenon may be lower than generally accepted. *Br J Anaesth* 1998; 80:255–256.
4. Chon D, Simon BA, Beck KC, et al. Differences in regional wash-in and wash-out time constants for xenon-CT ventilation studies. *Respir Physiol Neurobiol* 2005; 148:65–83.
5. Kreck TC, Krueger MA, Altemeier WA, et al. Determination of regional ventilation and perfusion in the lung using xenon and computer tomography. *J Appl Physiol* 2001; 91:1741–1749.
6. Hoffman EA, Reinhardt JM, Sonka M, et al. Characterization of the interstitial lung diseases via density-based and texture-based analysis of CT images of lung structure and function. *Acad Radiol* 2003; 10:1104–1118.
7. Drayer BP, Wolfson SK, Reinmuth OM, et al. Xenon enhanced CT for analysis of cerebral integrity, perfusion, and blood flow. *Stroke* 1978; 9:123–130.
8. Gupta R, Jovin TG, Yonas H. Xenon CT cerebral blood flow in acute stroke. *Neuroimaging Clin N Am* 2005; 15:531–42.
9. Lynch C, Baum J, Tenbrinck R. Xenon anesthesia. *Anesthesiology* 2000; 92:865–868.
10. Gur D, Drayer BP, Borovetz HS, et al. Dynamic computed tomography of the lung: regional ventilation measurements. *J Comput Assist Tomogr* 1979; 3:749–753.
11. Murphy DM, Nicewicz JT, Zabbatino SM, et al. Local pulmonary ventilation using nonradioactive xenon-enhanced ultrafast computed tomography. *Chest* 1989; 96:799–804.